

# The Cause of Photospheric and Helioseismic Responses to Solar Flares: High-Energy Electrons or Protons?

A. G. Kosovichev

*W.W.Hansen Experimental Physics Laboratory, Stanford University, Stanford, CA 94305, USA*

## ABSTRACT

Analysis of the hydrodynamic and helioseismic effects in the photosphere during the solar flare of July 23, 2002, observed by Michelson Doppler Imager (MDI) on SOHO, and high-energy images from RHESSI shows that these effects are closely associated with sources of the hard X-ray emission, and that there are no such effects in the centroid region of the flare gamma-ray emission. These results demonstrate that contrary to expectations the hydrodynamic and helioseismic responses ("sunquakes") are more likely to be caused by accelerated electrons than by high-energy protons. A series of multiple impulses of high-energy electrons forms a hydrodynamic source moving in the photosphere with a supersonic speed. The moving source plays a critical role in the formation of the anisotropic wave front of sunquakes.

*Subject headings:* Sun: flares – Sun: X-rays, gamma-rays – Sun: oscillations

## 1. Introduction

"Sunquakes", the helioseismic response to solar flares, are caused by strong localized hydrodynamic impacts in the photosphere during the flare impulsive phase. The helioseismic waves are observed directly as expanding circular-shaped ripples in SOHO/MDI Dopplergrams, which can be detected in Dopplergram movies and as a characteristic ridge in time-distance diagrams, (Kosovichev & Zharkova 1998; Kosovichev 2006a), or indirectly by calculating integrated acoustic emission (Donea et al. 1999; Donea & Lindsey 2005). Solar flares are sources of high-temperature plasma and strong hydrodynamic motions in the solar atmosphere. Perhaps, in all flares such perturbations generate acoustic waves traveling through the interior. However, only in some flares the impact is sufficiently localized and strong to produce the seismic waves with the amplitude above the convection noise level. It has been established in the initial July 9, 1996, flare observations (Kosovichev & Zharkova

1998) that the hydrodynamic impact follows the hard X-ray flux impulse, and hence, the impact of high-energy electrons. Nevertheless, a common paradigm is that the sunquake events are caused by accelerated protons because protons carry more momentum and penetrate deeper into the solar atmosphere than electrons, which lose most of their energy in the upper chromosphere. This paradigm is not easy to test because the gamma-ray emission, which indicates the presence of high-energy protons, is rarely observed.

In a large X17 flare of October 28, 2003, the gamma-ray emission observed by RHESSI was located close to the hard X-ray sources and two of the three places of the photospheric impacts (sunquake sources) (Kosovichev 2006a). Because of the close locations of the hard X-ray and gamma-ray sources these observations could not exclude the possibility of the proton or mixed electron-proton impacts (Zharkova & Zharkov 2007).

However, in one event, X4.8 flare of July 23, 2002, the hard X-ray and gamma-ray sources were significantly separated from each other. The centroid of the  $\gamma$ -ray 2.233 MeV neutron-capture emission was found to be displaced by  $20'' \pm 6''$  (with 5-sigma confidence) from that of the 0.3 – 0.5 MeV X-ray emission implying a difference in acceleration and/or propagation between the accelerated electrons and ions (Hurford et al. 2003). Therefore, this flare provides a unique opportunity to investigate the photospheric and helioseismic responses separately for high-energy electrons and protons. In this Letter, I present results of the analysis of the relationship between the hard X-ray and gamma-ray emissions and the hydrodynamic and seismic signals in the photosphere, using data from RHESSI (Lin et al. 2002) and MDI on SOHO (Scherrer et al. 1995). RHESSI provides X-ray/gamma-ray imaging spectroscopy from 3 keV to 17 MeV with angular resolution  $2.3'' - 3'$  ( $35''$  at gamma-ray energies) over the full Sun. MDI measures the Doppler velocity and the line-of-sight magnetic field of the photospheric plasma every minute with 2 arcsec/pixel resolution also over the full Sun.

## 2. Analysis of SOHO/MDI and RHESSI data

X4.7 flare of July 23, 2002, was the first flare, for which gamma-ray images were obtained (Hurford et al. 2003). Other examples of flares with RHESSI gamma-ray images are given by Hurford et al. (2006). The properties of the gamma-ray and hard X-ray emissions, and also other aspects of the July 23, 2002, flare, are discussed in the RHESSI special issue of ApJ Letters (v.595,no.2, 2003). The RHESSI observations revealed three hard X-ray sources and a gamma-ray source. Their positions in the MDI magnetogram are shown in Figure 1a (Krucker et al. 2003). The hard X-ray sources (marked as f1, f2 and f3) were located on both sides of the magnetic neutral line. The morphology of the gamma-ray emission was

not resolved but it could not have been more than 1 arcminute (FWHM) in extent and its centroid was  $20'' \pm 6$  south from the centroid of the hard X-ray sources and about  $30''$  from the f1 source.

The MDI Dopplergrams show strong impulsive variations close to the hard X-ray sources, but no impulsive variations in the region of the gamma-ray source centroid, or anywhere outside the hard X-ray sources. Figure 1b shows the positions of the impulsive Doppler velocity signals in the photosphere during the flare impulsive phase between 00:27 UT and 00:36 UT, July 23, 2002. This flare was rather close to the limb (coordinates of the flare sources are given in Fig. 1); the distance from the disk center was approximately 70 degrees. Thus, it is possible that the projection effect contributed to the opposite sign of the Doppler shift across the neutral line, if the angle between the magnetic field lines directing the plasma motion at the footpoints (Fig. 2) and the line of sight changes the sign. However, there might be other reasons related to flare hydrodynamics, which should be explored.

The strongest Doppler signal, corresponding to a downward plasma motion, appeared near the X-ray source, f1. Its position moved during the impulsive phase in the North direction. This motion is discussed in more detail in the next section. The time dependence of the velocity signal at source f1 corresponds very well (with the correlation coefficient of 0.8) to the total hard X-ray flux in the 50-300 keV range (Fig. 3c,d). The gamma-ray emission (Fig. 3e) is delayed by  $\sim 100$  sec because of the time for the neutrons to thermalize (Murphy et al. 2003).

The helioseismic waves are best visible at frequencies of about 5–6 mHz. To search for these waves the Dopplergrams were remapped into the heliographic coordinates, tracked to remove the displacement caused by the solar rotation, and then filtered using a band-pass filter centered at 5.5 mHz with a FWHM of 2 mHz. Then, the filtered Dopplergrams were remapped into the polar coordinates, centered at various points including all hard X-ray sources and the gamma source centroid region, and averaged azimuthally in several angular sectors. The averaged signals are plotted as a function of the radial distance and time, constituting time-distance propagation diagrams. The diagrams were inspected for an elongated characteristic ridge-like structure, which is caused by helioseismic waves as predicted by the theory (Kosovichev & Zharkova 1995), and observed in other sunquake events (Kosovichev & Zharkova 1998; Kosovichev 2006a). In this case, a rather weak ridge appeared only in the propagation diagram, which was centered in the region of the strongest impulsive Doppler signal at the f1 source and averaged in the North-West quadrant. It can be identified in Fig. 1c for distances between 20 and 40 Mm, just above the theoretical time-distance relation for helioseismic acoustic waves. The traveling wave front can be seen in the movie of the frequency-filtered Dopplergrams. The observed signal is rather weak because a

flare generates high-frequency acoustic waves, in which the plasma velocity is predominantly vertical (Kosovichev & Zharkova 1995), and its line-of-sight projection is reduced by almost 2/3 due to the close-to-limb location. The amplitude of the line-of-sight plasma velocity in this wave was about 20 m/s. For the other central positions (including X-ray sources f2 and f3, and X-ray and gamma-ray centroids) and sectors, the seismic waves were not detected. This analysis puts the source of the seismic wave within the lower red part of the Doppler source f1 in Fig. 1b. The start time estimated from the theoretical time-distance relation in the ray approximation is 00:28–00:30 UT. It is interesting that X-ray source f2 is marginally stronger than source f1, but the impulsive Doppler signal is stronger in the f1 position.

The close correlation of the hydrodynamic and helioseismic responses with the hard X-ray flux source and the absence of any significant photospheric signal in the region of the gamma-ray centroid provide evidence that the source of the helioseismic waves is associated with the high-energy electrons and not with the high-energy protons. We note that while the RHESSI data do not exclude the presence of protons in the footpoints of the hard X-ray sources, for this conclusion it is important that the proton flux in the gamma-ray centroid area was not weaker than that in the HRX sources. This assumption is supported by the RHESSI data. For further studies, it would be important to put precise limits on the proton flux at the X-ray footpoints and estimate the relative energetics of proton and electrons from RHESSI data.

### 3. Moving hard X-ray and sunquake sources

A characteristic feature of the seismic response in this flare and several others (Kosovichev 2006a,b) is anisotropy of the wave front: the observed wave amplitude is much stronger in one direction than in the others. In particular, the seismic waves excited during the October 28, 2003, flare had the greatest amplitude in the direction of the expanding flare ribbons. The wave anisotropy was attributed to the moving source of the hydrodynamic impact, which is located in the flare ribbons (Kosovichev 2006a,c). The motion of flare ribbons is often interpreted as a result of the magnetic reconnection processes in the corona. When the reconnection region moves up it involves higher magnetic loops, the footpoints of which are further apart. Of course, there might be other reasons for the anisotropy of the wave front, such as inhomogeneities in temperature, magnetic field, and plasma flows. However, the source motion seems to be quite important.

It is interesting that in the case of the July 23, 2002, flare the seismic source identified in MDI Dopplergrams as a place of strong Doppler shift in region f1 was moving mostly along the flare ribbon, and consequently the seismic wave had the strongest amplitude in

the direction close to the direction of the source motion (but not precisely; in this case, in addition to the other factors, stronger foreshortening on the East side might have contributed to the signal loss in the NE quarter). The Doppler source motion nicely corresponds to the motion of the hard X-ray source discovered by Krucker et al. (2003). Figure 4a shows the evolution of the hard X-ray sources, f1, f2 and f3, positions on the magnetogram; and Fig. 4b shows propagation diagrams for this sources determined by Krucker et al. (2003). From the top panel of Fig. 4b, the hard X-ray source, f1, traveled approximately 7 Mm in 5 min; this corresponds to the mean speed of approximately 20–25 km/s. The maximum speed according to Krucker et al. (2003) reached 50 km/s.

Using the MDI Dopplergrams, a similar time-distance propagation diagram was constructed for the plasma photospheric velocity along the line of motion of source f1. Figure 4c shows the Doppler velocity along a 2-pixel wide strip along this line. This diagram shows that the evolution of the hydrodynamic impact source is very similar to the evolution of the hard X-ray source (top panel in Fig. 4c). The mean speed of the hydrodynamic source was also about 20–25 km/s.

Therefore, we conclude that the seismic wave was generated not by a single impulse as was suggested in the sunquakes models of Kosovichev & Zharkova (1995); Medrek et al. (2000); Podesta (2005) but by a series of impulses, which produce the hydrodynamic source moving on the solar surface with a supersonic speed. The seismic effect of the moving source can be easily calculated by convolving the wave Green’s function (the wave signal from a point  $\delta$ -function type source),  $G(x - x_s, y - y_s, t)$  with a moving source function,  $S(x_s - V_x t, y_s - V_y t, t)$ . The results of these calculations are illustrated in Fig. 5, which shows the wave front for a source moving along the  $x$ -axis with a speed of 25 km/s. The strength of this source varied with time as a Gaussian with FWHM of 3 min (it is shown by black diamonds). The Green’s function was calculated by using the standard mode summation method (Kosovichev & Zharkova 1995). The strong anisotropy of the seismic wave is evident. Curiously, this effect is quite similar to the anisotropy of seismic waves on Earth, when the earthquake rupture moves along the fault (e.g. Ben-Menahem 1962). Thus, taking into account the effects of multiple impulses of accelerated electrons and moving source is very important for sunquake theories. These effects will be discussed in more detail in our future publications.

#### 4. Discussion

The analysis of RHESSI X-ray and gamma-ray images and SOHO/MDI Dopplergrams of the July 23, 2002, X4.8 solar flare revealed that the hydrodynamic and seismic responses

are closely associated the hard X-ray emission, both spatially and temporally, but showed no significant responses in the gamma-source centroid area. Because this flare was one of strongest gamma-flares, and the hard X-ray and gamma-ray sources were separated, these observations show that the accelerated protons are unlikely to be a source of the hydrodynamic response and sunquakes. Furthermore, the detailed analysis of the dynamics of sunquake sources in this Letter and in the paper by Kosovichev (2006a) reveals their close association with expanding flare ribbons and rapid HXR source motion along the ribbons, and, thus, with the magnetic reconnection process. The fast motion of these sources results in strong anisotropy of the seismic waves, clearly observed in the MDI data.

The general picture that comes from the analysis of MDI and RHESSI data is consistent with the previously developed hydrodynamic thick-target model, illustrated in Fig. 2 (Kostiuk & Pikelner 1975; Livshits et al. 1981; Fisher et al 1985; Kosovichev 1986). In this model, high-energy electrons heat the upper chromosphere to high temperatures generating a high-pressure region, expansion of which causes evaporation of the chromospheric plasma and a high compression shock. The shock reaches the photosphere and excites the seismic waves. However, the new results show that it is important to include effects of the multiple impact and moving source in the thick-target and sunquake models.

The photospheric and helioseismic effects observed during the impulsive phase of solar flares are closely related to the processes of acceleration and propagation of electrons and ions, and may provide new important information about these processes.

## REFERENCES

- Ben-Menahem, A. 1962, *J. Geophys. Res.*, 67, 345
- Donea, A.-C., Braun, D. C. & Lindsey, C., 1999, *ApJ*, 513, L143
- Donea, A.-C. & Lindsey, C., 2005, *ApJ*, 630, 1168
- Fisher, G. H., Canfield, R. C. & McClymont, A. N., 1985, *ApJ*, 289, 434
- Hurford, G. J., Schwartz, R. A., Krucker, S., Lin, R. P., Smith, D. M., & Vilmer, N. 2003, *ApJ*, 595, L77
- Hurford, G. J., Krucker, S., Lin, R. P., Schwartz, R. A., Share, G. H., & Smith, D. M. 2006, *ApJ*, 644, L93
- Kosovichev, A.G., 1986, *Bull. Crimean Astrophys. Obs.*, 75, 6
- Kosovichev, A. G. & Zharkova, V. V., 1995, *Seismic Response to Solar Flares: Theoretical Predictions*, in *Helioseismology. ESA SP, Proc. 4th Soho Workshop*, p.341
- Kosovichev, A. G. & Zharkova, V. V., 1998, *Nature*, 393, 317
- Kosovichev, A. G. 2006a, *Sol. Phys.*, 238, 1
- Kosovichev, A. G. 2006b, *Direct Observations of Acoustic Waves Excited by Solar Flares and their Propagation in Sunspot Regions*, in: *Solar MHD Theory and Observations: A High Spatial Resolution Perspective*, ASP Conference Series, Vol. 354, p.154
- Kosovichev, A. G. 2006c, *Sunquake sources and wave propagation*, in: *Proceedings of SOHO 18/GONG 2006/HELAS I, Beyond the spherical Sun*, ESA SP-624, p.134.1
- Kostiuk, N. D. & Pikelner, S. B., 1975, *Sov. Astr.*, 18, 590
- Krucker, S., Hurford, G. J., & Lin, R. P. 2003, *ApJ*, 595, L103
- Lin, R. P., et al. 2002, *Sol. Phys.*, 210, 3
- Livshits, M. A., Badalian, O. G., Kosovichev, A. G. & Katsova, M. M., 1981, *Sol. Phys.*, 73, 269
- Medrek, M., Murawski, K., & Nakariakov, V. 2000, *Acta Astronomica*, 50, 405
- Murphy, R. J., Share, G. H., Hua, X.-M., Lin, R. P., Smith, D. M., & Schwartz, R. A. 2003, *ApJ*, 595, L93

Podesta, J. J. 2005, Sol. Phys., 232, 1

Scherrer, P. H., et al. 1995, Sol. Phys., 162, 129

Zharkova, V. V., & Zharkov, S. I. 2007, ApJ, 664, 573



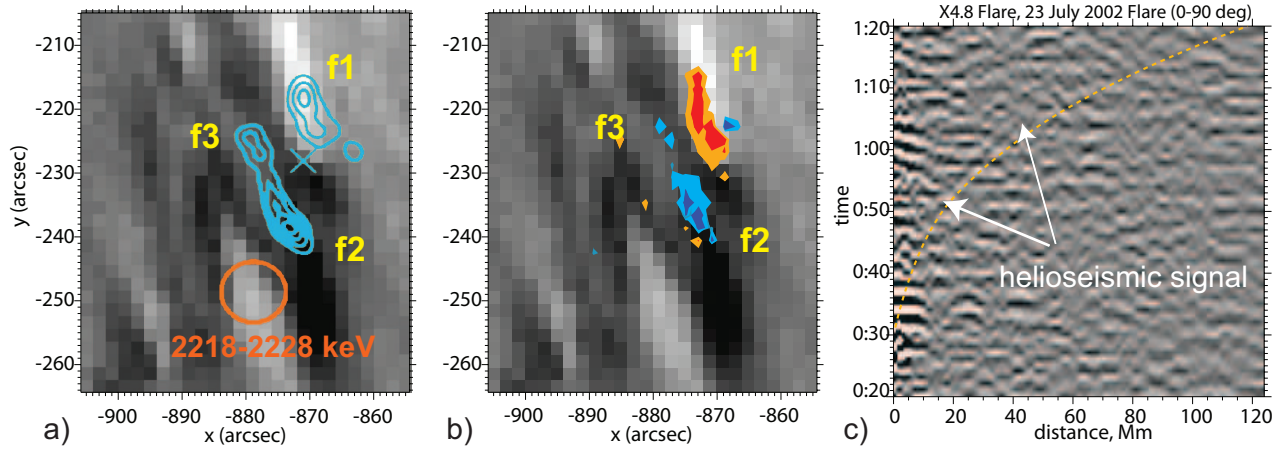


Fig. 1.— a) RHESSI observations of HXR (f1, f2, f3) sources (blue contours show the 50–100 keV map with 3'' resolution, and the blue cross shows the HXR centroid) and a gamma-ray source (orange circle shows the location of the gamma-ray centroid with  $1\sigma$  error) (from Krucker et al. (2003)). The gray-scale background is MDI magnetogram ( $\pm 600$  G range). b) MDI observations of Doppler velocity sources. Orange contour lines show positive (red-shift) velocity greater than 0.6 km/s; the red contours show 1 km/s; the blue contour lines show negative (blue-shift) velocity of -0.6 km/s, and dark blue shows -0.7 km/s. c) Time-distance map revealing a seismic wave front, which travels in the North-West direction from the location of source f1. The yellow dashed curve is a theoretical time-distance relation for helioseismic acoustic waves.

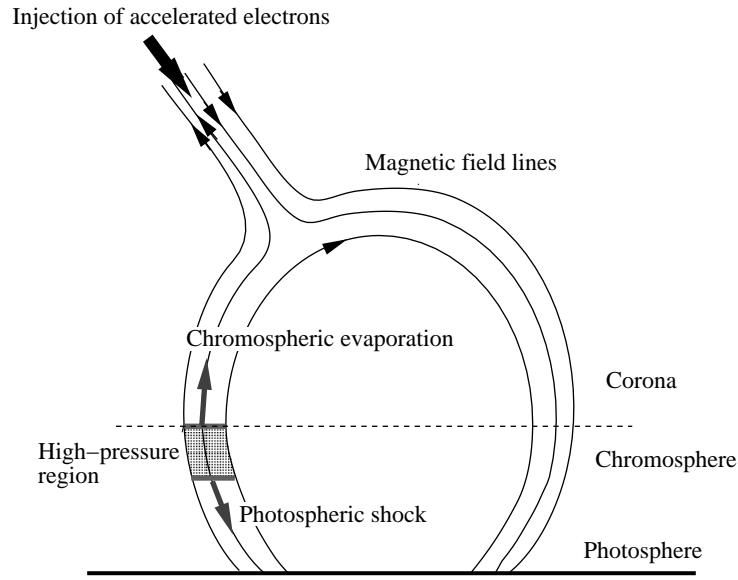


Fig. 2.— Illustration of the hydrodynamic thick-target model and the mechanism of sunquakes. High-energy electrons accelerated in the upper corona are injected along magnetic field lines into the atmosphere, generate a hard X-ray emission in the loop footpoints and heat the upper chromosphere to high temperature, producing a high-pressure region. The high-pressure region expands producing upward and downward propagating shocks. The downward shock reaches the photosphere and causes a sunquake.

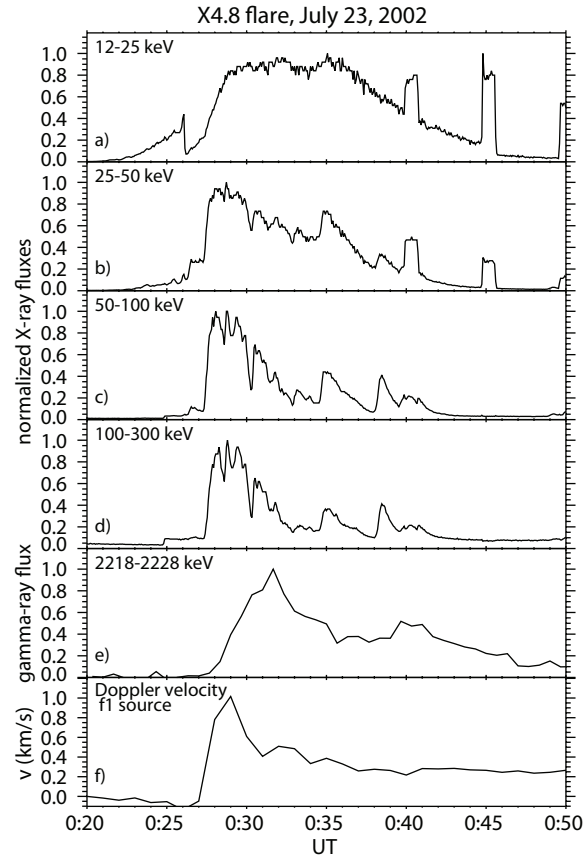


Fig. 3.— Integrated X-ray and gamma-ray fluxes, and Doppler shift in source f1 as a function of time.

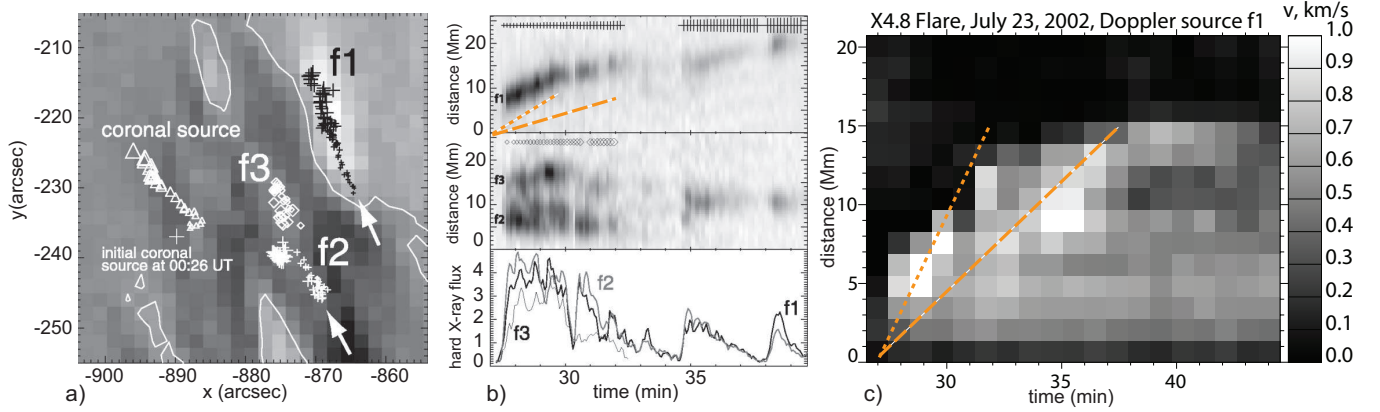


Fig. 4.— a) Evolution of HRX sources. The increasing size of the symbols represents times from 00:26:35 to 00:39:07 UT, and b) HXR profiles (black in the top two panels shows enhanced emission) along the ribbons, showing motion with speed of up to 50 km/s (from Krucker et al. (2003)). c) Doppler velocity profiles along the f1 ribbon, showing motion with averaged speed 25 km/s. The inclined orange lines correspond to 25 km/s (long dash) and 50 km/s (short dash).

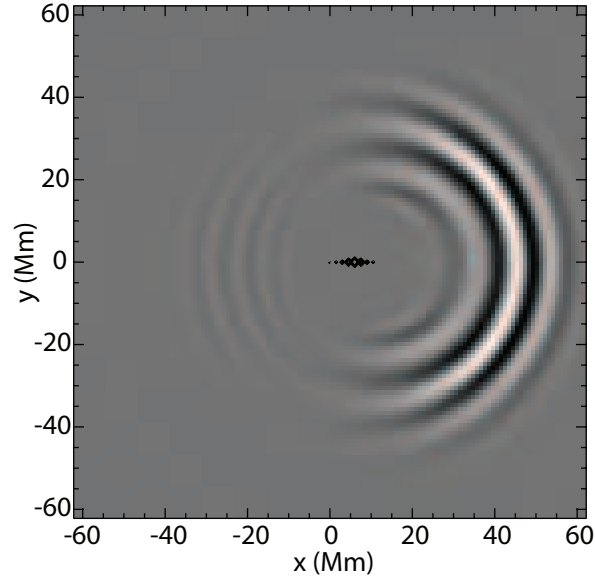


Fig. 5.— Theoretical model of seismic waves from a moving source, which explains the observed anisotropy of sunquakes. The point impulsive source is moving in the  $x$  direction with the constant speed of 25 km/s. Its strength as a function of time has a Gaussian shape with FWHM of 3 min. The locations of the source are shown by black diamonds at the center, the size of which is proportional to the source strength.